Which probes can report intrinsic dynamic heterogeneity of a glass forming liquid?

Keewook Paeng[1,2] and Laura J. Kaufman[1,a)]
[1]*Department of Chemistry, Columbia University, New York, New York 10027, USA*
[2]*Department of Chemistry, Sungkyunkwan University, Suwon 16419, South Korea*

(Received 5 July 2018; accepted 28 September 2018; published online 24 October 2018)

Using extrinsic probes to study a host system relies on the probes' ability to accurately report the host properties under study. Probes have long been used to characterize dynamic heterogeneity, the phenomenon in which a liquid near its glass transition exhibits distinct dynamics as a function of time and position, with molecules within nanometers of each other exhibiting dynamics that may vary by orders of magnitude. The spatial and temporal characteristics of dynamic heterogeneity demand the selection of probes using stringent criteria on their size and dynamics. In this report, we study the dynamic heterogeneity of the prototypical molecular glass former *o*-terphenyl by investigating single molecule rotation of two perylene dicarboximide probe molecules that differ in size and comparing this to results obtained previously with the probe BODIPY268. It is found that a probe's ability to accurately report dynamic heterogeneity in *o*-terphenyl depends on whether the reported distribution of dynamics overlaps with the intrinsic dynamics of the host, which is naturally related to the width of the intrinsic dynamics and the magnitude of dynamical shift in probe dynamics relative to the host. We show that a probe that rotates ≈15 times more slowly than the intrinsic dynamics of the host *o*-terphenyl senses the slowest ≈5% of the full dynamic heterogeneity whereas one that rotates ≈65 times more slowly than the host fails to report dynamic heterogeneity of the host. *Published by AIP Publishing.* https://doi.org/10.1063/1.5047215

I. INTRODUCTION

Given that glass formation is a kinetic process, characterizing and understanding the unusual dynamic phenomena that occur in the vicinity of the glass transition are crucial to understanding the properties of glass forming materials and the glass transition process itself. Key dynamic anomalies that occur near the glass transition temperature (T_g) include non-Arrhenius temperature dependences and non-exponential relaxations, and both have been heavily studied owing to their close and potentially causal relationship with the glass transition.[1–4]

Experimentally, monitoring rotations of fluorescent probes has been used to characterize molecular dynamics and mobility not only in glass formers near the glass transition but also near surfaces in thin films, in polymers during deformation, and in systems undergoing crystallization.[5–8] In many such studies, monitoring probe rotations has successfully revealed previously obscured dynamics. Inevitably, the success of such approaches relies on a probe's ability to track and report the dynamics of the host. Such ability is typically illustrated by showing that probe dynamics follow those of the host, with the relative relaxation time of the probe as a function of an external variable or through a particular process tracking that of the probe-free system.

It has been clearly demonstrated that using probe rotations to fully characterize dynamics in supercooled liquids and polymers comes with subtle challenges. In particular, it has been shown that the degree of non-exponentiality seen in probe rotational relaxation varies with the nature of the probe,[9] especially with the relaxation time of the probe relative to that of the host molecules.[10] This probe-dependent behavior is consistent with the understanding that non-exponential relaxations in systems near the glass transition are a manifestation of dynamic heterogeneity, a phenomenon in which molecular mobility in a given region at a given time may differ by orders of magnitude from regions potentially just nanometers away.[11]

Monitoring fluorescent probe rotations at a single molecule level has been considered an ideal tool for investigating dynamic heterogeneity, as it has the known strengths of rotational probe measurements but avoids ensemble averaging that complicates the analysis of heterogeneous systems.[12–18] Despite this promise, in analogy to findings in ensemble measurements, it is now appreciated that single molecule rotational experiments are not generically suitable for characterizing dynamic heterogeneity in supercooled liquids, and the ability of a probe to track the dynamics of a supercooled host with temperature is necessary but insufficient to assure that the probe can report on dynamic heterogeneity in the system.[13] Indeed, different single molecule probes that track host temperature dependence have reported different degrees of heterogeneity in a given host, with slowly rotating (typically large) probes suggesting that the host was less heterogeneous than more quickly rotating probes.[19,20] This finding, mirroring

a)Author to whom correspondence should be addressed: kaufman@chem.columbia.edu

earlier findings in ensemble studies, was recognized and then exploited to characterize time scales over which the regions of distinct dynamics exist in liquids and polymers near the glass transition. Later, "ideal probes"—single molecule probes that could report the full breadth of dynamic heterogeneity in a system—were described and employed towards the same end.[21,22]

In this paper, we present a probe-dependent study comparing single molecule rotational dynamics measurements as a reporter of underlying host dynamic heterogeneity in supercooled *o*-terphenyl. The probes used are BODIPY268 and two probes with perylene diimide cores, N,N′-dipentyl-3,4,9,10-perylenedicarboximide (pPDI) and N,N′-bis(2,5-di-tert-butylphenyl)-3,4,9,10-perylenedicarboximide (tbPDI). Previously, we showed that BODIPY268 not only tracked *o*-terphenyl dynamics with temperature but also could report the full breadth of heterogeneity in that system, thus identifying this molecule as an ideal probe for that host.[21] This was similarly demonstrated for pPDI in polystyrene.[22] The third probe, tbPDI, was used in earlier studies of *o*-terphenyl and glycerol as one of a set of probes with perylene diimide cores; it was shown that tbPDI was not an ideal reporter of dynamic heterogeneity in *o*-terphenyl owing to a combination of its limited photostability and its slow rotation relative to the host molecule.[19,20] The current study updates our understanding of the circumstances under which particular probes can report aspects of dynamic heterogeneity and the methods by which one establishes whether a probe can report the full breadth of heterogeneity of a particular host.

II. EXPERIMENTAL APPROACH

A. Sample preparation

To remove impurities, *o*-terphenyl (Sigma-Aldrich) was re-crystallized at least three times in methanol and dissolved in toluene at the concentration of 5 mg/ml. The solutions were then photobleached in a homebuilt, high power light emitting diode (LED) based photobleaching setup for 48 h to achieve fluorescent-free host matrices.[23] Silicon wafer substrates (6.5 × 6.5 mm) were used to avoid dewetting of the film during sample preparation at room temperature, where the room temperature is ≈50 K above T_g. Piranha solution (H_2SO_4:H_2O_2 = 3:1) cleaned substrates were treated with trichloro(phenethyl)silane chloroform solution, which results in a hydrophobic surface. The fluorescent probes used were pPDI (Sigma-Aldrich), tbPDI (Sigma-Aldrich), and BODIPY268, which was synthesized as described in Ref. 21. The fluorescent probe solutions with a concentration on the order of 10^{-10} M in toluene were mixed (≈1:200 dilution) with the host solution and solvent-casted onto the silicon wafer. The typical film thickness was 300–500 nm, as confirmed by ellipsometry (J.A. Woollam, alpha-SE). The concentrations of the probe in the hosts were on the order of 10^{-10} M, which results in 100 to 200 molecules per field of view.

B. Imaging

Rotation of probe molecules in the host matrix was studied using a homebuilt microscope in a wide-field configuration. A vacuum cryostat (Janis, ST-500) was used for temperature and environment control with a typical pressure of ≈1 mTorr. Excitation of the fluorescent probes was achieved by using a continuous wave laser (Nd:Vanadate) with an excitation wavelength of 532 nm. Light was directed to a multimode fiber (Newport, F-MCB-T-1FC) on a speaker-based homebuilt fiber shaker and then focused onto the back of the objective lens (Zeiss, LD Plan-Neofluar, air 63×, NA = 0.75) to create a randomly polarized, homogeneously illuminated field of view of ≈100 μm in diameter. Fluorescence was collected with the same objective lens and passed through a dichroic mirror. Long-pass and band-pass filters were used to further isolate probe emission. A Wollaston prism (Karl Lambrecht, MW2S-12-5-HEAR400-700) split the image into two orthogonal polarizations that were imaged onto an electron multiplying charge-coupled device camera (Andor iXon DV887).

Typical excitation power at the back of the objective lens was 10-15 mW, which corresponds to a power density of ≈100-150 W/cm^2 at the sample. Specifically, power of 15 (10) mW was used for the temperature-dependent measurements of pPDI (tbPDI). For additional measurements, excitation power was varied to control the time to photobleaching and the trajectory length of the measurement. For pPDI, the longest trajectory length data set was collected with an excitation power of 2.5 mW, whereas the shortest trajectory length set was collected at 120 mW excitation power. For tbPDI, data sets of two different trajectory lengths were collected, the shorter at 10 mW and the longer at 5 mW. The frame rate was deliberately controlled to be between 15 and 20 frames per median rotation time (τ_{fit}) so that the measurement could capture rotation times, approximately ten times faster than the median rotation time, while maximizing the trajectory length of the measurement. Movies with frame rate >5 Hz were collected continuously, whereas slower frame rate movies were collected with 0.2 s constant exposure time, with illumination shuttered between frames to limit photobleaching.

Measurement temperatures reported in this study are the estimated temperatures of the sample, which accounts for heating of the sample by the excitation beam. As previously reported, an excitation power dependence study at constant set temperature of tbPDI in *o*-terphenyl showed that the rotational correlation time changes by −0.01 decades/mW and −0.0012 decades/mW for continuous and shuttered measurements, respectively.[22] The changes in rotational correlation time were converted to temperature changes using the temperature dependence of the dielectric relaxation time of *o*-terphenyl that results in sample independent temperature correction factors of 0.042 K/mW and 0.0048 K/mW for continuous and shuttered measurements, respectively.

C. Data analysis

Single molecule linear dichroism analysis was performed using a custom program written in IDL (Interactive Data Language, ITT Visual Information Solutions), as described in detail in Ref. 24. Analysis began with identifying the positions of each single molecule in a band-passed and 500 frames summed image. From the identified positions, the polarized

fluorescence intensities (I_s(t), I_p(t)) of each molecule were extracted from raw images for all the frames in a movie. Single molecule linear dichroism [$LD(t) = (I_s - I_p)/(I_s + I_p)$] trajectories were then calculated, and linear dichroism autocorrelations of $LD(t)$ were constructed via $C(t) = [\sum_{t'} a(t') \cdot a(t' + t)]/[\sum_{t'} a(t') \cdot a(t')]$, where $a(t) = LD(t) - \langle LD(t) \rangle$. Constructed autocorrelations of each molecule were fit to a stretched exponential function ($C(t) = C(0) \cdot \exp[-(t/\tau_{fit})^{\beta}]$), which returned the fit values of $C(0)$, τ_{fit}, and β. The related quantity, rotational correlation time, τ_c, was calculated from the fit values of τ_{fit} and β via $\tau_c = (\tau_{fit}/\beta) \cdot \Gamma(1/\beta)$, where Γ is the gamma function. Fitting the autocorrelation decays was done with a least squares fitting algorithm until the correlation decayed to 0.1 with constraints of $0.2 < \beta < 2.0$, $0.3 < C(0) < 2.0$, frames/$\tau_{fit} > 2$, and trajectory length $>10\ \tau_{fit}$. Quasi-ensemble autocorrelations (ACF_{QE}) were constructed by averaging the single molecule autocorrelation decays. The $ACFs_{QE}$ were also fit to stretched exponential decays, yielding $\tau_{fit,QE}$, β_{QE}, and $\tau_{c,QE}$.

III. RESULTS

A. Relaxation is slaved to host dynamics for all probes

Assessing the suitability of a probe to study aspects of host dynamics typically involves showing that the probe is slaved to the host, as assessed by following probe dynamics as a function of an external variable, such as temperature, or through a process, such as crystallization. For studying dynamics in the supercooled regime, monitoring the temperature dependence of the probe is appropriate: host dynamics change precipitously as temperature decreases, and any potential probe of supercooled liquid dynamics must track this change.

Here, we examine this behavior for three probes—BODIPY268, pPDI, and tbPDI—in *o*-terphenyl. While assessing whether these probes track *o*-terphenyl dynamics can be achieved via ensemble measurements, given the ultimate goal of using these probes as single molecule reporters of local environments, we do so using single molecule data. In the presence of sufficiently long trajectories, two approaches beginning with single molecule data can be and were used to assess rotational correlation time (τ_c) as a function of temperature for each probe. First, each single molecule ACF was constructed: at least 1000 molecules of each probe at each temperature were analyzed to help ensure that the full distribution of time scales was captured. From here, either each single molecule ACF can be fit to a stretched exponential function or the single molecule ACFs can be averaged into a single, quasi-ensemble ACF (ACF_{QE}) that is fit to a stretched exponential function ($C(t) = C(0) \cdot \exp[-(t/\tau_{fit})^{\beta}]$). In both cases, τ_{fit}, β, and τ_c values are obtained, with a QE subscript denoting those obtained from the ACF_{QE}. In general, τ_{fit} describes the time scale on which an ACF initially decays to 1/e of the initial autocorrelation value (C(0)) and β describes the degree of stretching in the decay. τ_c has contributions from both τ_{fit} and β and captures the area under the correlation function: as such, it corresponds to the average rotational correlation (or relaxation) time experienced by the probe. The distribution of τ_c values from single molecule ACFs can be assembled, and the median τ_c can be extracted. Alternately, τ_c can be extracted from the ACF_{QE}. Median τ_c obtained from single molecule distributions and $\tau_{c,QE}$ obtained from the ACF_{QE} as a function of temperature for the three probes in *o*-terphenyl are shown in Fig. 1. Measurements span slightly over two orders of magnitude in τ_c. In all cases, constraints on frame rate and experimental setup stability set the lower and upper bounds of τ_c measured, respectively. The particular host and probe properties set the temperature range that can be probed, with typical values between 1.00 and 1.06 T_g. Full single molecule distributions of τ_{fit}, β, and τ_c and additional data set characteristics at each temperature for pPDI and tbPDI are given in Fig. S1 and Tables S1 and S2, while those for BODIPY268 are presented in Ref. 21.

The temperature dependences of rotational correlation times of BODIPY268, pPDI, and tbPDI probes in *o*-terphenyl

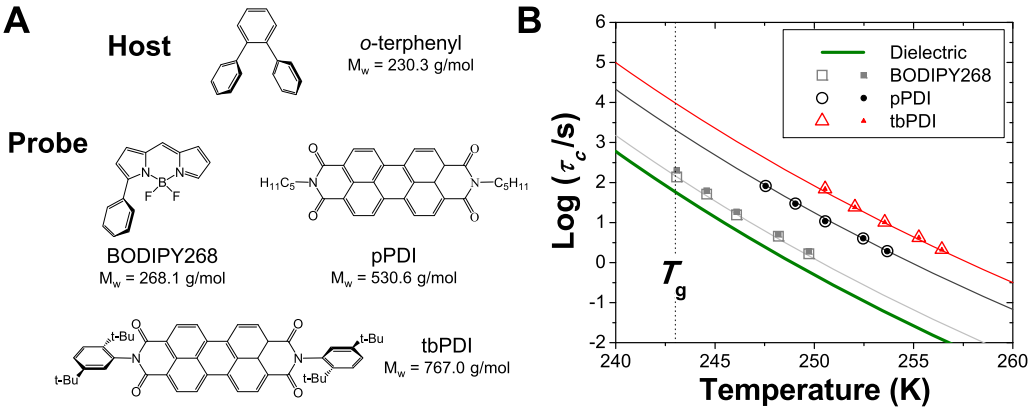

FIG. 1. (a) Chemical structures and molecular weights of the fluorescent probes and the host molecule, *o*-terphenyl. (b) Temperature dependence of rotational correlation time (τ_c) for BODIPY268 (squares), pPDI (circles), and tbPDI (triangles) in *o*-terphenyl compared with that of dielectric relaxation (green line, from information provided in Ref. 25). The data from BODIPY268 were also presented in Ref. 21. Solid symbols are median single molecule τ_c values obtained from single molecule ACFs, and open symbols are $\tau_{c,QE}$ obtained from $ACFs_{QE}$. The solid lines through the data are vertical shifts of the dielectric relaxation line. While τ_c values are not sensitive to trajectory length, we note that median trajectory lengths in terms of probe τ_{fit} value for the data presented are 173 $\tau_{fit,med}$, 264 $\tau_{fit,med}$, and 227 $\tau_{fit,med}$ for BODIPY268, pPDI, and tbPDI, respectively.

are presented in Fig. 1. BODIPY268 data were also presented in Ref. 21. The solid curves are the Vogel Fulcher Tammann (VFT) fits ($\log(\tau/\tau_0) = B/(T - T_0)$) to the dielectric relaxation data for *o*-terphenyl with T_0 = 168 K, $\log(\tau_0) = -22.5$, and B = 1820 K as in Ref. 25 shifted to match the rotational correlation times of each probe molecule. Each probe reproduces the strong temperature dependence of the dielectric relaxation of *o*-terphenyl, which emphasizes (1) that the system under study is in the supercooled regime and non-exponential relaxations can be assumed to emerge from the supercooled nature of the system rather than from other possible sources[26] and (2) the validity of the probe approach to studying dynamic properties of glass formers near the glass transition temperature. The vertical shifts of the VFT curve are 0.4, 1.55, and 2.22 decades for BODIPY268, pPDI, and tbPDI, respectively, indicating that the rotational dynamics of the probes are 2.5, 35.6, and 166.0 times slower than those of *o*-terphenyl as measured through dielectric relaxation. We note that in earlier results, we reported tbPDI to show rotational dynamics 297 times slower than the host *o*-terphenyl.[19] We attribute the difference to improvements made to the experiment since the earlier report, with the current experiment having (1) more molecules analyzed and (2) less sample to sample variability in τ_c for a particular set temperature due to improved consistency in attaining good contact between the sample and heating elements in the cryostat.

The time scale of BODIPY268 rotational relaxation relative to dielectric relaxation matches that of tetracene, which has nearly the same molecular weight (228.3 g/mol) as the host *o*-terphenyl (230.3 g/mol) and also matches the *o*-terphenyl self-rotation time scale, as reported by NMR measurements;[9,27] this suggests that the BODIPY268 probe rotates with nearly the same rate as *o*-terphenyl molecules, while the other two probes are notably slower.

B. Degree of non-exponentiality in relaxation differs between probes

A more rigorous test of whether a particular probe can be used to study dynamics in supercooled liquids is whether the probe captures the dispersion or heterogeneity of relaxation time scales present. Regardless of whether such non-exponentiality emerges from relaxations distributed in space or time, the ACF_{QE} obtained from probe molecules should return the same β value as a probe-free ensemble, as this observable reconstructs the ensemble and does not privilege spatial or temporal heterogeneity. For the three probes studied here, stretched exponential fits of the quasi-ensemble correlation functions of BODIPY268, pPDI, and tbPDI probes in *o*-terphenyl did not vary with temperature [Figs. 2(a)–2(c)], and best fit β_{QE} values once combined across temperatures were β_{QE} = 0.63, 0.93, and 0.96, respectively [Fig. 2(d)].

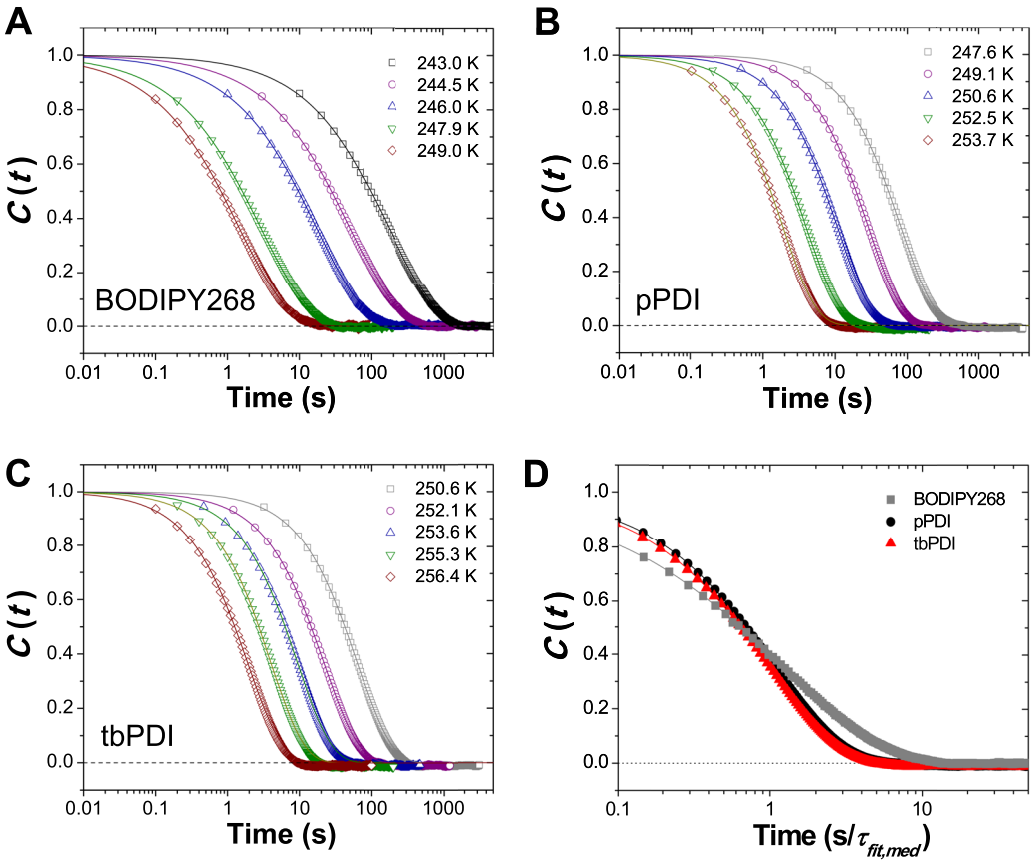

FIG. 2. Normalized quasi-ensemble autocorrelation functions of (a) BODIPY268 (also presented in Ref. 21), (b) pPDI, and (c) tbPDI probes in *o*-terphenyl for the temperatures indicated (open symbols). The solid lines are best-fits to stretched exponential functions. (d) Quasi-ensemble ACF curves for all temperatures combined for each probe. The data presented here have median trajectory lengths of 173 $\tau_{fit,med}$, 264 $\tau_{fit,med}$, 227 $\tau_{fit,med}$, and β_{QE} values of 0.63, 0.93, and 0.96 for BODIPY268, pPDI, and tbPDI, respectively.

Temperature combined ACFs were obtained by rescaling time by $\tau_{fit,med}$ (for each probe and temperature) for each data set. We note that while the temperatures investigated were not identical for each probe, at most temperatures studied, at least two of the three probes were monitored and different probes return different β values at the same temperature.

As for τ_c, β can be obtained not only from the ACF_{QE} but also from single molecule ACFs. For the measurements shown here, median single molecule β values (β_{med}) were 0.67, 0.95, and 0.97 for BODIPY268, pPDI, and tbPDI, respectively. (The data for pPDI and tbPDI are shown in Figs. S1E and S1F and Tables S1 and S2; BODIPY268 data are in Ref. 21.) We note that in contrast to β_{QE}, β_{med} would report different results in the limit of purely spatial and purely temporal heterogeneity, with β_{med} returning 1 for static heterogeneous relaxation distributed in space (with a corresponding broad array of τ_c values representing distinct dynamics in different regions of the sample). By contrast, β_{med} would be the same as β_{QE} if the typical single molecule experiences and reports various dynamic environments in the system, as would occur in the case of a system in which ergodicity is restored on the time scale of the experiment. Using BODIPY268 in *o*-terphenyl, we previously showed that for sufficiently long trajectories, β_{med} is the same value as β_{QE}. Below, this is now shown for the PDI probes.

In a system in which ergodicity can be restored, if a particular probe molecule has not been observed sufficiently long for the dynamics to have randomized, that molecule will have a β value that is higher than β_{QE}: this would apply also to β_{med} if the population of single molecules is not tracked for sufficiently long times. The evolution of the distribution of single molecule β values with trajectory length is shown for the three probes in Fig. 3. It is evident that for each probe the median of the distribution moves to lower values and the distribution narrows as trajectories get longer. Because pPDI is the most photostable of the probes, its trajectories are longest (in terms of τ_{fit}, or the number of probe rotations). Despite this, at the longest trajectories measured for each probe, BODIPY268 has the lowest β_{med} value, and it is the only probe with β_{med} nearly equal to the ensemble result in probe-free experiments. The results from simulations of homogeneous rotational diffusion, which may also lead to a broad distribution of β values for short trajectories, are shown in the supplementary material for trajectory lengths equal to the longest achieved for each of the three probes (Fig. S2). It can be appreciated that β distributions that peak at values <1 are inconsistent with homogeneous rotational diffusion even when finite trajectory length effects lead to significant broadening.[28]

The difference between β_{med} values as a function of probe and trajectory length can be more fully appreciated by binning data as a function of trajectory length more finely and analyzing median β values as a function of trajectory length within and across data sets (Fig. 4). As is evident from the BODIPY268 probe data (light gray symbols), as trajectory length increases, β_{med} decreases from close to one and converges to the β_{QE} value, which represents the full set of dynamic environments that the probe can access and report. This trend is consistent with the view of an ergodic system: each molecule in a dynamically heterogeneous system resides in a single dynamic region for some amount of time ($\beta \approx 1$); as the observation time—or trajectory length—increases, the molecule experiences additional dynamical environments, resulting in a decreasing single molecule β value that ultimately converges to the ensemble β value, indicating recovered ergodicity of the system. For BODIPY268 in *o*-terphenyl, β_{med} deviates from 1 by $\approx 25\tau_{fit,con}$ and approaches a value near β_{QE} by $\approx 500\tau_{fit,con}$. This suggests that initial changes in dynamics (dynamical exchange or exchange time) occur by approximately 25 times the host structural relaxation time, and the time required to recover ensemble averaged relaxation for a typical single molecule is hundreds of times the host structural relaxation time.

While each probe returns β_{med} equal to β_{QE} at the longest trajectories, only BODIPY268 returns β values close to those obtained from ensemble probe-free experiments. The fact that each probe returns a different β, the barometer of dynamic heterogeneity, underscores that careful selection of the probe molecule is needed when studying dynamic heterogeneity. This difference across probes and the persistence of high β

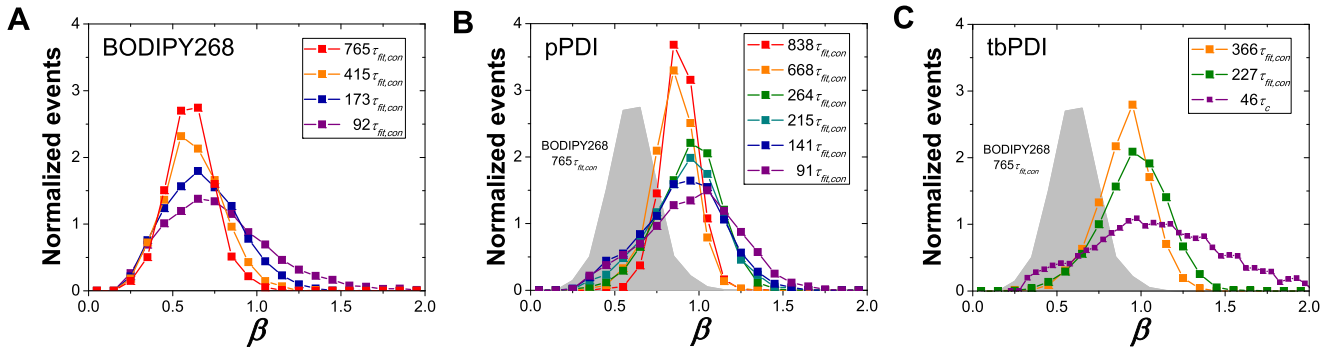

FIG. 3. Distributions of single molecule β values with varying median trajectory length for (a) BODIPY268, (b) pPDI, and (c) tbPDI probes in *o*-terphenyl. Trajectory lengths are expressed in terms of $\tau_{fit,con}$, which is the median τ_{fit} value of the longest trajectory length data set, where the τ_{fit} value has converged and shows no additional trajectory length dependence. Distributions are normalized by the area under the curve. Filled gray distributions in (b) and (c) are the longest trajectory length β distribution (765 $\tau_{fit,con}$) of BODIPY268. Distributions in green in (b) and (c) are also shown in Fig. S1E and Fig. S1F. Distributions in (a) are also shown in Ref. 21, and distribution in purple in (c) is obtained from Ref. 19. Additional characteristics of data sets as a function of trajectory length for pPDI and tbPDI are given in Table S3.

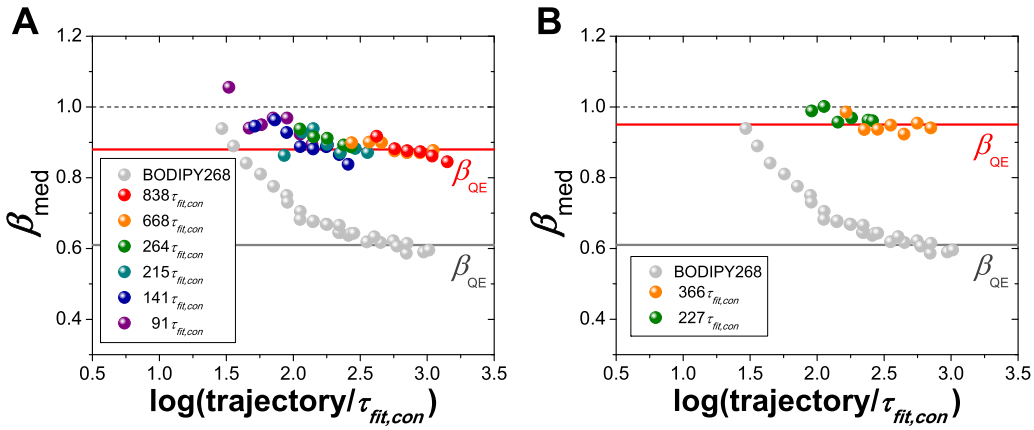

FIG. 4. Trajectory length dependence of β_{med} for subsets of (a) pPDI and (b) tbPDI data sets together with β_{QE} (solid red line) for these probes. Different color symbols represent subsets produced from the indicated trajectory length data sets, each of which is divided into subsets of 0.1 decade intervals. Each point in the figure represents the β_{med} value from at least 200 molecules. Gray points and lines are the results from BODIPY268 in *o*-terphenyl, which are also presented in Ref. 21. The horizontal lines are probe-specific β_{QE} values obtained from the longest trajectory length data set for each probe.

values for single PDI molecules even for long trajectories suggests not that these probes are in single dynamic environments but rather that they reside in and average over multiple dynamic domains. This is directly related to the fact that pPDI and tbPDI rotate 14 times and 66 times more slowly, respectively, than the BODIPY268 probe that has nearly identical dynamics as the host *o*-terphenyl.

C. Role of probe and host dynamics in reporting dynamic heterogeneity

To further investigate why PDI molecules cannot report the full set of dynamic environments in the host, inverse Laplace transform (ILT) analysis was performed on the single molecule data. The procedure is fully elaborated in Ref. 21, and some key details are provided in the supplementary material. In brief, the ILT of a stretched exponential function can be expressed by Eq. (1), which assumes that a stretched exponential form results from a superposition of exponential relaxations with different relaxation times. The distribution $P(\log\tau; \tau_{fit}, \beta)$ can be numerically obtained for any τ_{fit} and β values and reflects the distribution of exponential relaxations that constitute the stretched exponential function,

$$\exp\left[-\left(t/\tau_{fit}\right)^{\beta}\right] = \int_{-\infty}^{\infty} P(\log\tau; \tau_{fit}, \beta)\cdot\exp(-t/\tau)d\log\tau. \quad (1)$$

ILT analysis is illustrated for pPDI in *o*-terphenyl. First, from an ACF_{QE} measurement of pPDI in *o*-terphenyl, the expected exponential relaxation distribution is numerically obtained. While there is very limited trajectory length dependence of ACF_{QE} (Table S3), we use the longest trajectory length data (838 $\tau_{fit,con}$) for this analysis and thus perform the ILT analysis on $P(\log\tau; \tau_{fit} = 1, \beta = 0.88)$. This distribution is shown as the red line in Fig. 5 and is termed the ILT distribution. To test whether the measured single molecule ACFs also return this distribution, each single molecule ACF is also "unwrapped" through an ILT as described by Eq. (1). This distribution (medium gray in Fig. 5), termed the *ILT-built* distribution, is the full set of exponential relaxation times that the probe molecules report in space and time during the experiment. This distribution roughly matches the ILT distribution associated with a stretched exponential function with β = 0.88, the β_{QE} value of pPDI in *o*-terphenyl. A match of the ILT and *ILT-built* distribution shows that the ACF_{QE} and the single molecule ACFs equally well capture the probe-accessed dynamic heterogeneity despite the fact that single molecule ACFs suffer from more statistical noise than the ACF_{QE}.

To more fully understand why each probe reports different β_{med} and β_{QE} values even for long trajectories, we compare the *ILT-built* distributions of the three probes in *o*-terphenyl (Fig. 5). The pPDI and tbPDI distributions are shifted on the τ-axis according to the vertical shifts of the temperature

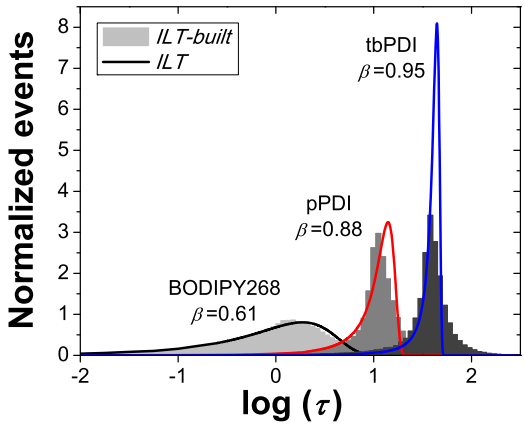

FIG. 5. ILT distributions (solid lines: black for BODIPY268, red for pPDI, and blue for tbPDI) and *ILT-built* distributions (light gray for BODIPY268, medium gray for pPDI, and dark gray for tbPDI). The data in this figure are from the longest trajectory length sets collected 765 $\tau_{fit,con}$, 838 $\tau_{fit,con}$, and 366 $\tau_{fit,con}$ for BODIPY268, pPDI, and tbPDI, respectively. pPDI and tbPDI distributions are shifted on the x-axis according to the vertical shifts of the temperature dependence of τ_{fit} relative to the BODIPY268 temperature dependence. BODIPY268 data was also presented in Ref. 21, but with the ILT distribution of β = 0.61, which is the β_{QE} of the longest trajectory length examined rather than of β = 0.65 as used in the earlier work.

dependence of τ_{fit} relative to the BODIPY268 temperature dependence. Here we use shifts in τ_{fit} rather than τ_c since the shift in τ_c value (shown in Fig. 1) takes into account contributions from β values that separately contribute to the *ILT-built* distributions.

As BODIPY268 reports a β_{QE} value that is close to that reported by the self-rotation of *o*-terphenyl, it is reasonable to assume that the ILT associated with $\beta = 0.61$ represents the full breadth of relaxation times present in the *o*-terphenyl. For the pPDI probe, the shape of the *ILT-built* and ILT distributions do not match as well as in the case of BODIPY268, but the width of the *ILT-built* distribution of pPDI presented in Fig. 5 (FWHM = 0.29) matches with that of the ILT distribution of $\beta = 0.88$ (FWHM = 0.29). This implies that although pPDI does not report the full breadth of relaxations present in the *o*-terphenyl, as also indicated by the high β_{QE} value, the measured single molecule τ_{fit} and β distributions of pPDI at this trajectory length (838 $\tau_{fit,con}$) reflect dynamic heterogeneity sensed by the pPDI probes. For tbPDI, the β_{QE} value near unity together with the mismatch in the *ILT-built* and ILT distributions suggest that this probe has very limited ability to report dynamic heterogeneity in *o*-terphenyl and furthermore that the τ_{fit} and β distributions of tbPDI as obtained from single molecule ACFs are not the result of dynamic heterogeneity but instead are dominated by statistical effects (as also suggested by Fig. S2).

We suggest the reason that pPDI can report a subset of the dynamic heterogeneity in *o*-terphenyl while tbPDI cannot is related to the overlap of the ILT distributions with the native relaxation time distribution of the host. The ILT distribution of pPDI overlaps with the ILT distribution of BODIPY268 over ≈0.9 decades, which equates to ≈5% of the probability distribution (Fig. 5). This suggests the pPDI probes can sense the slowest 5% of the *o*-terphenyl dynamic heterogeneity. The overlap between the ILT distribution of tbPDI and BODIPY268 is negligible (≈0.3%), making tbPDI ill-suited as a reporter of dynamic heterogeneity of *o*-terphenyl. Additional insight into how slower probe rotation affects β values can be gleaned from considering earlier simulations investigating how time scales and distributions of time scales of host relaxation and dynamic exchange (exchange time) give rise to particular stretching exponent behavior.[29] Here, systems with exchange times on average ten times longer than the host rotational correlation time showed β_{med} values that evolved similarly to the BODIPY268 in *o*-terphenyl data, evolving from near 1 at short trajectories to the β_{QE} (≈0.65 in the simulated case) associated with the full breadth of dynamic heterogeneity by $100\tau_c$ (or 10 times the characteristic exchange time, τ_{ex}). For a system where the ratio of average exchange time to rotational correlation time was an order of magnitude less (=1), β_{med} showed very little evolution with trajectory length, decreasing only to $\beta_{QE} \approx 0.9$ (vs. 0.65). This shift in ratio of exchange time to rotational correlation time mimics that in the experimental data here. Here, because the host is fixed, the exchange time is fixed. The relevant relaxation times to consider in the experiment are those of the probes. We posit that the exchange time of the host must be approximately 10 times longer than the rotational correlation rate of the probe for the probe to report the full breadth of dynamic heterogeneity. The divergence of the BODIPY268 β_{med} value from 1 at $\approx 25\tau_{fit}$ suggests that typical time between environmental exchange in *o*-terphenyl in this temperature regime is ≈25 times the host relaxation time, and the resulting ratio of exchange time to probe rotation is greater than 10. For pPDI, which rotates ≈15 times more slowly than BODIPY268 (or *o*-terphenyl itself), the ratio is decreased by a factor of 15 to well below 10, resulting in significant time averaging that manifests in only a modest decrease in β_{med} as a function of observation time.

IV. CONCLUSION

A probe's ability to report dynamic heterogeneity of the prototypical molecular glass former *o*-terphenyl was studied by changing probe size and rotation time relative to the host molecule. It is shown that the shift in the rotation time correlates with the magnitude of the deviation of the probe stretching exponent β relative to that of the host. This is true independent of trajectory length for β_{QE} and at long trajectories for median β values obtained from single molecule autocorrelations. The expected full distribution of rotation times in the system reported by the probe was estimated from the inverse Laplace transform (ILT) of the quasi-ensemble stretched exponential decay of the probe and compared with the distribution extracted from the single molecule measurements through summing up the ILT of individual single molecule decays (*ILT-built*). Matching ILT and *ILT-built* distributions confirm that the dynamics reported in single molecule experiments are the result of dynamic heterogeneity of the host, and the overlap between the host native dynamics and probe as represented by the ILT controls the probe's ability to report dynamic heterogeneity of the system. It is suggested that (1) the wider the host ILT (the lower the host β), (2) the smaller the shift in rotational dynamics of the probe relative to those of the host, and (3) the lower the ratio of the rotational correlation time of the probe to the exchange time of the host, the greater the ability of the probe to report the dynamic heterogeneity of the system. In *o*-terphenyl, BODIPY268 captures the full width of the dynamic heterogeneity, whereas the ≈15 times more slowly rotating pPDI senses the slowest ≈5% of full dynamic heterogeneity. The ILT of the ≈65 times more slowly rotating tbPDI probe neither overlaps with that of the host nor matches the *ILT-built* distribution, confirming that tbPDI is not a suitable probe for studying dynamic heterogeneity of *o*-terphenyl. Beyond the particular probe/host combinations measured here and elsewhere, it is now clear that to characterize dynamic heterogeneity in a system with an extrinsic probe, the suitability of a given probe to study a given host system can be evaluated through ensemble or single-molecule experiments. Before proceeding to labor-intensive single molecule measurements that may characterize length and time scales associated with dynamic heterogeneity of a particular host, ensemble measurements with the same probe can be performed. If such measurements do not return the β value that is known to characterize the host system from probe-free experiments, the probe is unable to report the full breadth of dynamic heterogeneity at a single molecule level and should not be further used in attempts to do so.

SUPPLEMENTARY MATERIAL

See supplementary material for one figure and two tables detailing pPDI and tbPDI data collected as a function of temperature and associated with Figs. 1 and 2, one table detailing pPDI and tbPDI data collected as a function of trajectory length associated with Figs. 3 and 4, a figure showing β distributions associated with homogeneous rotational diffusion as a function of trajectory length, and information about simulations and *ILT-built* distribution construction.

ACKNOWLEDGMENTS

We thank Alyssa Manz for assistance with simulations of homogeneous rotational diffusion. This work was supported by NSF Nos. CHE 1213242 and CHE 1660392.

[1]L. Berthier and G. Biroli, Rev. Mod. Phys. **83**, 587 (2011).
[2]D. Cangialosi, J. Phys.: Condens. Matter **26**, 153101 (2014).
[3]F. H. Stillinger and P. G. Debenedetti, Annu. Rev. Condens. Matter Phys. **4**, 263 (2013).
[4]K. L. Ngai, J. Non-Cryst. Solids **275**, 7 (2000).
[5]H. N. Lee, K. Paeng, S. F. Swallen, and M. D. Ediger, Science **323**, 231 (2009).
[6]K. Paeng, H. N. Lee, S. F. Swallen, and M. D. Ediger, J. Chem. Phys. **134**, 024901 (2011).
[7]K. Paeng, C. T. Powell, L. Yu, and M. D. Ediger, J. Phys. Chem. Lett. **3**, 2562 (2012).
[8]K. Paeng, S. F. Swallen, and M. D. Ediger, J. Am. Chem. Soc. **133**, 8444 (2011).
[9]M. T. Cicerone, F. R. Blackburn, and M. D. Ediger, J. Chem. Phys. **102**, 471 (1995).
[10]L. M. Wang and R. Richert, J. Chem. Phys. **120**, 11082 (2004).
[11]M. D. Ediger, Annu. Rev. Phys. Chem. **51**, 99 (2000).
[12]L. J. Kaufman, Annu. Rev. Phys. Chem. **64**, 177 (2013).
[13]K. Paeng and L. J. Kaufman, Chem. Soc. Rev. **43**, 977 (2014).
[14]L. A. Deschenes and D. A. Vanden Bout, J. Phys. Chem. B **106**, 11438 (2002).
[15]R. Zondervan, F. Kulzer, G. C. G. Berkhout, and M. Orrit, Proc. Natl. Acad. Sci. U. S. A. **104**, 12628 (2007).
[16]A. Schob, F. Cichos, J. Schuster, and C. von Borczyskowski, Eur. Polym. J. **40**, 1019 (2004).
[17]A. N. Adhikari, N. A. Capurso, and D. Bingemann, J. Chem. Phys. **127**, 114508 (2007).
[18]H. Uji-i, S. M. Melnikov, A. Deres, G. Bergamini, F. De Schryver, A. Herrmann, K. Mullen, J. Enderlein, and J. Hofkens, Polymer **47**, 2511 (2006).
[19]L. M. Leone and L. J. Kaufman, J. Chem. Phys. **138**, 12a524 (2013).
[20]S. A. Mackowiak, L. M. Leone, and L. J. Kaufman, Phys. Chem. Chem. Phys. **13**, 1786 (2011).
[21]K. Paeng, H. Park, D. T. Hoang, and L. J. Kaufman, Proc. Natl. Acad. Sci. U. S. A. **112**, 4952 (2015).
[22]K. Paeng and L. J. Kaufman, Macromolecules **49**, 2876 (2016).
[23]T. K. Herman, S. A. Mackowiak, and L. J. Kaufman, Rev. Sci. Instrum. **80**, 016107 (2009).
[24]D. T. Hoang, K. Paeng, H. Park, L. M. Leone, and L. J. Kaufman, Anal. Chem. **86**, 9322 (2014).
[25]R. Richert, J. Chem. Phys. **123**, 154502 (2005).
[26]D. A. Turton and K. Wynne, J. Chem. Phys. **131**, 201101 (2009).
[27]I. Chang, F. Fujara, B. Geil, G. Heuberger, T. Mangel, and H. Sillescu, J. Non-Cryst. Solids **172-174**, 248 (1994).
[28]C.-Y. Lu and D. A. V. Bout, J. Chem. Phys. **125**, 124701 (2006).
[29]K. Stokely, A. S. Manz, and L. J. Kaufman, J. Chem. Phys. **142**, 114504 (2015).